Efficient dye removal by Streptomyces cyaneus lacasse heterologously expressed within S. cerevisiae cell walls immobilized within tyramine-modified alginate beads using visible light photopolymerization

Dragana Josić Stanić
Innovative Centre of the Faculty of Chemistry, University of Belgrade
Nikolina Popović Kokar
University of Belgrade Faculty of Chemistry: Univerzitet u Beogradu Hemijski fakultet
Anja Stošić
University of Belgrade Faculty of Chemistry: Univerzitet u Beogradu Hemijski fakultet
Milica Crnoglavac Popović
University of Belgrade Faculty of Chemistry: Univerzitet u Beogradu Hemijski fakultet
Olivera Prodanović
University of Belgrade Institute for Multidisciplinary Research: Univerzitet u Beogradu Institut za multidisciplinarna istrazivanja
Goran Vladisavljević
: Loughborough University Department of Chemical Engineering
Radivoje Prodanović
rprodano@chem.bg.ac.rs

University of Belgrade Faculty of Chemistry: Univerzitet u Beogradu Hemijski fakultet
https://orcid.org/0000-0003-4662-1825

Research Article

Keywords: tyramine-alginate laccase, yeast surface display, immobilization, riboflavin, visible light photopolymerization, dye removal

Posted Date: February 13th, 2024

DOI: https://doi.org/10.21203/rs.3.rs-3838408/v1

Abstract

Environmental pollution by synthetic dyes presents serious global problem, since they are not biodegradable in conventional anaerobic wastewater treatment. Many studies using enzymatic degradation of synthetic dyes, especially laccases were reported. For the lacasse immobilization, hydrogels obtained through UV photopolymerization have been commonly used. However, cross-linking with visible light presents a less harmful and invasive method with possible applications in tissue engineering. In this study, laccase from *Streptomyces cyaneus* was expressed on the surface of yeast cell walls, followed by cell lysis and immobilization within modified alginate beads. The resulting laccase biocatalysts were additionally crosslinked using visible light in the presence of riboflavin as a photoinitiator. Photopolymerization was confirmed by FTIR spectroscopy. The obtained biocatalysts with improved pH and temperature stability were obtained. At 60 °C, cell wall-immobilized laccase entrapped in photopolymerized tyramine-alginate hydrogel showed 30% higher enzymatic activity compared to the non-photopolymerized tyramine-alginate biocatalyst, and 250% higher activity compared to the biocatalyst immobilized in native alginate beads. Photopolymerized biocatalysts were tested for the decolorization of different classes of synthetic dyes. The relative decolorization of Evans Blue and Remazol Brilliant Blue by photopolymerized biocatalysts reached 75% and 77%, respectively, without the addition of redox mediators.

Introduction

The use of synthetic dyes in the chemical and textile industry is of great importance, resulting in the annual production of over 700 000 tons of various dyes and pigments worldwide (Uygun et al. 2021). The most industrially used synthetic dyes can be classified as azo dyes, anthraquinone, triphenylmethane, and indigo dyes according to the main structure which often includes chromophores (-C = C-, -C = O, -C = N-, $-NO_2$, -N = N- and quinonoid rings) responsible for absorption of visible light (Legerska et al. 2016). Among the synthetic dyes, azo dyes are the most widely used dyes, because they are structurally diverse, of high quality, and account for more than half of the total world synthetic dye production (Strong &Claus 2011). Industrially produced dyes are generally considered xenobiotic compounds, so it is unsurprising that they are not biodegradable in conventional anaerobic wastewater treatment plants. The resistance of synthetic dyes to biological degradation processes leads to significant groundwater and river contamination, posing a serious environmental problem (Stolz, 2001). Azo dyes are characterized by one or more azo groups (-N = N-) connecting differently substituted aromatic rings (Popli & Patel 2015). This complex structure with aromatic substitutions forms a conjugated system (chromophore) responsible for enhanced water solubility and resistance to degradation under natural conditions (Khan et al., 2013, Shanmugam et al. 2012). Azo dyes are electron-deficient compounds that can be degraded via azo reduction, but toxic products are obtained, while the environmentally more acceptable method is degradation through oxidation (Brown et al. 1993, Hsueh et al. 2009). The efficiency of degradation and initial rate of color removal depends on the electron-donating properties of the substituents on the phenolic ring and their relative position about the azo bond (Li et al. 1999, Strong & Claus 2011). Most of

the methods described in the literature for synthetic dye removal, including chemical, physical, electrochemical, and biological approaches, are generally ineffective and uneconomical (Uygun et al. 2021). However, phenoloxidases (peroxidases, laccases, and tyrosinases) were recognized early, with laccase showing the greatest potential for application (Strong & Claus 2011).

Laccase (benzendiol: oxygen oxidoreductase, EC 1.10.3.2) is an extracellular glycoprotein enzyme, that belongs to the group of multiple copper protein family, that include ferroxidases, ceruloplasmin, ascorbate oxidase, and bilirubin oxidase (Hoegger et al. 2006, Li et al. 1999). Laccases originate from various bacteria, fungi, and higher plants, and can be found even in larval and adult cuticles of insects. They have several biological roles that include lignification, delignification, detoxification, pathogenicity, morphogenesis, sporulation, and others. Laccase has found wide applications in biotechnology, due to its low substrate specificity, utilization of oxygen as the final electron acceptor, and lack of requirement for cofactors or peroxides (Strong & Claus 2011, Uygun et al. 2021). Laccases catalyze the oxidation of a large number of aromatic compounds such as di- and polyphenols, aminophenols, polyamines, lignins, aryl diamines, methoxyphenols, aromatic amines, ascorbate, benzenethiols, metal ions (Mn^{2+}) and organometallics (e.g. $[W(CN)_8]^{4-}$, $[Fe(EDTA)]^{2-}$) (Fernández-Fernández et al. 2013, Mate & Alcalde 2017). The laccase molecule in the active center contains 4 copper atoms, classified into three groups (a type-1, a type-2, and two type-3 coppers) associated with three redox sites. The first step of the laccase catalytic mechanism involves the oxidation of the substrate at the first redox site and simultaneous reduction of T1Cu, after which electrons are transferred to the trinuclear cluster, formed by the copper atoms in the second (T2Cu) and third (T3Cu) redox sites. This trinuclear cluster is where O_2 is reduced to two water molecules (Hakulinen & Rouvinen 2015). Due to their ability to oxidize a wide range of compounds using only oxygen as a secondary substrate, laccases are excellent biocatalysts from biotechnological and environmental perspectives. However, the industrial-scale application of laccases is limited due to low stability, short service life, difficult reuse, and high price (Fernández-Fernández et al. 2013, Zhou et al. 2021). The problem of enzyme production on a larger scale has been overcome through gene cloning, enzyme overexpression, and directed in vitro evolution (Strong & Claus 2011). One of the ways to overcome the mentioned limitations and enable the industrial-scale application of enzymes is their immobilization.

Enzyme immobilization refers to the physical confinement of enzymes within a defined space, along with enhancing their catalytic characteristics such as activity, selectivity, specificity, improved pH and temperature stability, and resistance to inhibitors (Taheri-Kafrani et al. 2021). One of the main advantages of enzyme immobilization is the increased recycling efficiency, allowing the enzyme to be reused in multiple catalytic cycles without significantly losing its unique properties (Bilal et al. 2019). Laccase immobilization has been extensively studied using different approaches including physical or chemical interactions like entrapment (matrix encapsulation) within (bio)polymeric hydrogels crosslinked by bi-functional reagents, adsorption on glass and alginate beads, or covalent binding to an insoluble supporting matrix like silica gel (Bilal et al. 2019, Daâssi et al. 2014). The use of natural polysaccharides (alginate, chitosan, modified cellulose, agar) as carriers for enzyme immobilization is simple, eco-friendly,

cost-effective. It causes relatively little damage to the native structure of the enzyme (Daâssi et al. 2014, Shokri et al. 2021).

Alginate is a natural, linear anionic polysaccharide, obtained from brown seaweed algae, composed of alternating blocks of α-L-guluronate (G) and β-D-mannuronate (M) residues connected by (1, 4) glycosidic linkages. The ability of alginate to form hydrogels in the presence of divalent cations (Ca^{2+}, Mg^{2+}) under very mild conditions suitable for living cells along with its non-toxicity, biodegradability, structural similarity to extracellular matrices of living tissues and the possibility of chemical modification, makes it an excellent material for laccase entrapment. (Lee & Mooney 2001, Lee & Mooney 2012, Pawar & Edgar 2012, Popović et al. 2021) Immobilizing enzymes in ionically crosslinked macro-beads leads to leakage of laccase (Prodanovic et al. 2015). Also, the mechanical properties of ionically crosslinked polymers (such as elastic modulus and swelling ratio) are generally poor. Hence, ionic crosslinking is often insufficient and should be supplemented by covalent crosslinking, which can be achieved through chemical modification of the functional groups of natural polymers (-OH, -COOH, and -NH2) (Chen et al. 2021, Sakai et al. 2007). Therefore, in this research, alginate was first oxidized with sodium periodate. Reductively aminated with tyramine hydrochloride, and finally crosslinked simultaneously by ionic and covalent bonds using visible light photopolymerization for covalent crosslinking.

Photo-crosslinked modified alginate hydrogels are useful in biomedical applications, primarily in tissue engineering, wound healing, regenerative medicine, controlled drug delivery, and 3D bioprinting (Chiulan et al. 2021, Higham et al. 2014, Mishbak et al. 2019). The use of UV-cross-linkable hydrogels as injectable materials for soft tissue regeneration has faced challenges in clinical translation due to concerns about their biosafety when exposed to UV light. UV light has the potential to generate reactive oxygen species (ROS) that can cause DNA damage, leading to accelerated tissue aging or an increased risk of cancer (Bryant et al. 2000, Noshadi et al. 2017). Studies have shown that UV light at a wavelength of 337 nm can induce oxidative DNA alterations. Still, the extent of DNA damage decreases significantly when the light wavelength is above 470 nm (Kong et al. 2009, Noshadi et al. 2017). The use of visible light and safer photoinitiators in synthesizing hydrogels enhances their effectiveness in biocatalysts immobilization and tissue engineering. Visible light is less detrimental to proteins, DNA and cell structures. It penetrates more deeply with lower energy compared to UV light (Dahle et al. 2005) making it suitable for minimally invasive in situ crosslinking of injectable hydrogel materials (Noshadi et al. 2017). Multiple studies have documented that visible light, in the presence of riboflavin as a photoinitiator, can trigger the gelation of polymers modified with tyramine (Donnelly et al. 2017). When choosing photoinitiators, the main concern is the cytotoxicity of free radicals produced by their photolysis. One of the advantages of riboflavin (vitamin B2) as a photoinitiator is its biocompatibility, water solubility, and low toxicity. Unlike some traditional photoinitiators that may raise concerns about their safety in biomedical applications, riboflavin is naturally present in many foods. It has been extensively studied for its beneficial effects on health (Kim & Chu 2009).

This study aimed to achieve the expression of active laccase derived from *Streptomyces cyaneus* 3335 by effectively binding it to the surface of *Saccharomyces cerevisiae* EBY100 cells. Furthermore, we have

enhanced the laccase activity by inducing cell lysis and obtaining yeast cell walls with significantly increased laccase activity. Alginate, a natural heteropolysaccharide, was successfully modified by tyramine and the production of modified polymer was optimized and confirmed using UV-Vis, FTIR, and ^{1}H NMR spectroscopic methods. Subsequently, the successful immobilization of laccase within calcium-tyramine-alginate beads was performed to obtain a biocatalyst with improved characteristics and the ability for repeated use. The ability of Ca^{2+}-tyramine-alginate hydrogel beads loaded with laccase immobilized on yeast cell walls to undergo photopolymerization in the presence of the riboflavin photoinitiator under visible light was demonstrated for the first time. The impact of photopolymerization on the pH and temperature stability of the immobilized biocatalyst and its activity was investigated based on the decolorization of Amido Black 10B, Evans Blue, Remazol Brilliant Blue, Guinea Green and Methylene Blue.

Materials and methods

Chemicals

Alginic acid-sodium salt from brown algae, tyramine-hydrochloride, and photoinitiator riboflavin (vitamin B2) were purchased from Sigma Aldrich (St. Louis, MO, USA). Sodium cyanoborohydride was purchased from Merck (Darmstadt, Germany), and sodium metaperiodate from VWR Chemicals (Leuven, Belgium). Calcium chloride, sodium-chloride, and cooper sulfate pentahydrate were purchased from Betahem (Belgrade, Serbia), while substrate for laccase, 2,2-azino-bis-(3-ethylbenzothiazoline-6-sulphonic acid) (ABTS), was supplied from AppliChem (Darmstadt, Germany). The agar for medium preparation was ordered from Torlak (Serbia), while yeast nitrogen base without ammonium sulfate and amino acids (YNB) and casamino acids (CAA) were ordered from Roth (Karlsruhe, Germany). The synthetic dyes were purchased from Roth (Karlsruhe, Germany) and Sigma (St. Louis, MO, USA). All other chemicals were of analytical reagent grade or higher and supplied by Sigma-Aldrich.

The production of laccase in Saccharomyces cerevisiae EBY100 strain

The gene for laccase from *Streptomyces Cyaneus* strain was synthesized by GenScript (Piscataway, USA) and cloned into the pCTCON2 vector by Selin Ece and colleagues (Donnelly et al. 2017). The *Saccharomyces cerevisiae* strain and the plasmid vector pCTCON2 were obtained from Professor Dane Wittrup (MIT, Boston, USA).

Transformation of competent Saccharomyces cerevisiae cells

The gene for laccase was cloned into the pCTCON2 vector and the empty pCTCON2 vector without the laccase gene was used to transform competent yeast cells. Initially, the transformation of competent *E. coli* cells (XL10 Gold) with the genetic constructs was performed, followed by plasmid isolation, DNA verification through gel electrophoresis, and subsequent use to transform pre-prepared competent *S. cerevisiae* cells. The competent S. cerevisiae cells were thawed on ice, centrifuged (2 min at 6000 rpm),

and the supernatant was discarded. The pellet was then resuspended in a 50% solution of PEG 3350 (260 µL), followed by the addition of lithium acetate (36 µL), ssDNA (50 µL; 2 mg/mL), and plasmid DNA (14 µL). The mixture was incubated at 42 ℃ for 1 h. Transformed *S. cerevisiae* EBY100 cells were seeded in YNB-CAA glucose medium (final glucose concentration of 2% (w/v)) supplemented with adenine (final concentration of 0.2 mg/mL), and incubated at 30 ℃ and 180 rpm for 16 h.

Surface expression in yeast cells

Once the OD600 reached 5, laccase expression was induced by transferring the cells to YNB-CAA galactose medium (final galactose concentration of 2% (w/v)) supplemented with adenine (final concentration of 0.2 mg/mL), with an initial OD600 of 0.5, and incubating them at 28 ℃ and 180 rpm for 16 h. After expression, the cells were washed three times with sodium acetate buffer (0.1 M, pH 4.5), and their activity was measured following the procedure described in Section Determination of laccase enzyme activity on the surface of yeast cells.

Yeast cell lysis with an organic solvent

To increase the activity of surface-expressed yeast cell laccase, cells were lysed using a 3% toluene solution in water (4.11 g of cells in 30 mL of 3% toluene solution). The lysis process was carried out at 25 ℃ for 24 h, which was determined as the optimal lysis time. Lysis was halted by centrifugation (15 min at 3000 rpm), followed by washing with sodium acetate buffer (0.1 M, pH 4.5) until all traces of toluene were removed. The lysed cells were then incubated at 25 ℃ for 1 h in a solution containing Cu^{2+} (2 mM), and their activity was measured using the method described in Section Determination of laccase enzyme activity on cell walls.

Determination of laccase enzyme activity on the surface of yeast cells

The determination of laccase enzyme activity on the yeast cell surface was performed at room temperature using ABTS (a model substrate for laccase, ε_{405} = 36,000 M^{-1} cm^{-1}). The oxidation of ABTS was monitored by measuring the absorbance at 405 nm using an Elisa Microplate Reader. For the measurement of laccase activity expressed on the surface of yeast cells, a reaction mixture consisted of sodium acetate buffer (1092 µL; 0.1 M, pH 4.5), cell suspension (8 µL; 250 mg/mL) and $CuSO_4 \times 5H_2O$ solution (200 µL; 20 mM) in the same buffer. This reaction mixture was transferred to a microplate (200 µL), followed by ABTS (50 µL, 20 mM) addition to the final concentration of 5 mM. The absorbance at 405 nm was then measured every 15 min at room temperature for 1 h.

Determination of laccase enzyme activity on cell walls

The assay for measuring the activity of laccase expressed on cell walls consisted of sodium acetate buffer (1092 µL; 0.1 M, pH 4.5), cell wall suspension (8 µL; 150 mg/mL), and $CuSO_4 \times 5H_2O$ solution (200 µL; 20 mM) in the same buffer. The resulting reaction mixture was transferred to a microplate (200 µL),

followed by the addition of ABTS (50 µL, 20 mM), (final concentration was 5 mM). The absorbance at 405 nm was then measured every minute at room temperature for 8 min.

Modification of alginate with tyramine

Alginate was dissolved in distilled water at a final concentration of 1.12% (w/v). Sodium metaperiodate was added to the alginate solution at varying concentrations (1.25 mM, 2.5 mM, 5.0 mM, and 7.5 mM) to achieve the molarity ratios of periodate to alginate glycoside units of 2.5 mol%, 5 mol%, 10 mol%, and 15 mol%. The periodate oxidation reaction occurred in the dark at + 4°C for 24 h and was stopped by adding glycerol (500 mM) and stirring for 30 min. The oxidized alginate was then precipitated using 1% sodium chloride (w/v) and two volumes of 96% ethanol (v/v). This precipitation process was repeated twice after dissolving the alginate in water at a final concentration of 1% (w/v). The resulting precipitate was separated, air-dried, and dissolved in sodium-phosphate buffer (0.1M, pH 6) at a final concentration of 1% (w/v). Solid tyramine hydrochloride was added to the solution at 1.5% (w/v) final concentration (86 mM) followed by the addition of solid sodium cyanoborohydride at a final concentration of 0.5% (w/v). The reaction mixture was stirred in the dark at room temperature for 24 h. At the end of the reaction, modified alginate was precipitated by adding sodium chloride to 1 M final concentration and two volumes of 96% (v/v) ethanol. Afterward, the precipitate was dissolved in water (1%, w/v) and underwent two additional precipitation steps using the same procedure. The modified tyramine-alginate was lyophilized and stored at -20°C.

Spectral characterization of modified alginate

Modified and unmodified alginates were dissolved in distilled water at a final concentration of 0.1% (w/v) for UV-Vis spectral characterization. UV-Vis spectra were obtained using an LLG-uniSPEC2 spectrophotometer, in the wavelength range from 200 to 330 nm. IR spectra of alginates were collected using a Thermo Scientific Nicolet 6700 FT-IR spectrometer with attenuated total reflectance (ATR) technique in the mid-IR range (1800 – 600 cm^{-1}). 1H NMR spectra were recorded on a Bruker Avance III 500 MHz instrument with deuterium oxide as the solvent. Chemical shifts in NMR are reported in parts per million (δ) relative to tetramethyl silane as the internal standard.

Immobilization of cell wall laccase in alginate and tyramine-alginate beads

Among the modified alginates, the one with 2.5 mol% and 5 mol% modification was selected due to its balanced viscosity and degree of modification. Highly modified alginates led to lower solution viscosity due to bond breakage during periodate oxidation, making them unsuitable for forming mechanically stable spherical beads. According to that, native alginate and tyramine-alginate were suspended in a sodium-acetate buffer (0.1 M, pH 4.5) in different concentrations according to the degree of modification. A 4.8% (w/v) solution of native alginate, an 8.8% (w/v) solution of tyramine-alginate with 2.5 mol% modification, and a 10.2% (w/v) solution of tyramine-alginate with 5 mol% modification were prepared. The cell walls containing laccase were prepared in the same buffer, at a concentration of 600 mg/mL. The prepared solutions of alginate/tyramine-alginate and laccase cell walls were combined in a

volumetric ratio of 3:1. This resulted in a final mixture containing 3.25 (w/v) native alginate, 6.8% (w/v) of 2.5 mol% tyramine-alginate, 7.8% (w/v) of 5 mol% tyramine-alginate (w/v) and 150 mg/mL yeast cell walls with laccase with each polymer. The mixture was then added dropwise into a 6% $CaCl_2$ solution while continuously stirring on a magnetic stirrer for 30 minutes. Finally, the beads were stored in a sodium-acetate buffer (0.1 M, pH 4.5) containing a Ca^{2+} (5 mM) solution at a temperature of 4°C. All bead preparations were conducted in triplicate, and subsequent measurements were carried out using these beads.

Photopolymerization of biocatalysts with visible light

Yeast cell walls immobilized in native alginate, 2.5 mol% and 5 mol% tyramine-alginate were incubated in riboflavin photoinitiator solutions. The incubation was performed using 0.005% (w/v) and 0.01% (w/v) riboflavin solutions in sodium phosphate buffer (0.1 M, pH 6), and the beads were incubated for 15 min. After incubation, the beads were subjected to photopolymerization using visible light in a customized photoreactor (green LED lights) for 30 min, at a distance of 2 cm from the light source. This allowed for photopolymerization and additional cross-linking of the hydrogel. Subsequently, the beads were rinsed multiple times with sodium acetate buffer (0.1 M, pH 4.5) containing Ca^{2+} (5 mM) and stored in the same buffer at + 4°C.

Characterization of the immobilized cell wall laccase

Characterization of dual-crosslinked tyramine-alginate beads prepared by a two-step crosslinking process (ionically and photochemically with visible light)

Spectral analysis of cell walls with surface displayed laccase immobilized in modified alginate was challenging due to the complexity of the structure. To confirm the success of photopolymerization, spectral characterization of tyramine-alginate beads crosslinked ionically, as well as ionically and photochemically, was performed, without immobilized laccase cell walls. A solution of 5 mol% modified tyramine-alginate was prepared in sodium acetate buffer (0.1 M, pH 4.5) with a final concentration of 7.8% (w/v) and then added dropwise into a 6% $CaCl_2$ solution while continuously stirring on a magnetic stirrer for 30 minutes. The beads were then incubated in a 0.01% (v/w) riboflavin solution for 15 min. After incubation, the beads were exposed to visible light for 30 min using a customized photoreactor equipped with green LED lights, maintaining a distance of 2 cm from the light source. The photopolymerized beads were washed several times with Na-acetate buffer (0.1 M, pH 4.5) containing Ca^{2+} (5 mM) and were lyophilized. IR spectra of alginates were collected using a Thermo Scientific Nicolet 6700 FT-IR spectrometer with attenuated total reflectance (ATR) technique in the mid-IR range ($1800 - 600\ cm^{-1}$).

Determining the enzymatic activity of immobilized laccase on yeast cell walls

The determination of the enzymatic activity of alginate beads with immobilized laccase cell walls was performed by adding the beads to a mixture consisting of sodium acetate buffer (200 µL; 0.1 M, pH 4.5), $CuSO_4 \times H_2O$ solution (50 µL, 20 mM) and ABTS solution (250 µL, 20 mM) in the same buffer (final concentration of ABTS was 10 mM). Every 10 min, 200 µL of the reaction mixture was taken, and the absorbance at 405 nm was measured at room temperature. Immediately after measuring the absorbance, 200 µL of the solution was returned to the beads. The change in absorbance was monitored after a certain time from the addition of ABTS due to the hindered diffusion of the substrate within the beads. When determining the enzymatic activity of all samples, measurements were performed in triplicate.

Temperature stability

The temperature stability of both free and immobilized laccase was evaluated by subjecting them to different temperatures (25, 30, 60, 65, and 80°C) for a duration of 1 h in the optimal buffer. Based on the obtained results after 1 h of incubation at 60 ℃, the temperature stability of the immobilized enzyme was investigated at the same temperature (60 ℃) over an extended incubation period (2, 4, and 6 h). Following the incubation period, the free or immobilized enzyme was cooled on ice for 5 min, and the enzyme activity was measured using the procedure described above. The residual activity of differently immobilized enzyme, incubated at various temperatures, was normalized to the activity of laccase immobilized with the native non-photopolymerized alginate at room temperature and presented as residual activity.

pH stability

The pH stability of immobilized yeast cell walls with surface-displayed laccase was determined by incubation in the optimal sodium acetate buffer (0.1 M, pH 4.5) for 0, 24, 72 h, and 21 days at room temperature. After the incubation period, the enzyme activity was measured relative to the activity of laccase immobilized within native non-photopolymerized alginate at the start of the incubation period (0 h) and presented as residual activity.

Dye decolorization

Photopolymerized and non-photopolymerized Ca-tyramine-alginate beads with immobilized laccase cell walls were investigated for their ability to decolorize various synthetic dyes: Amido Black 10B, Evans Blue, Remazol Brilliant Blue, Guinea Green, Methylene Blue, and Methyl Green. Stock solutions of the dyes were prepared in sodium acetate buffer (0.1M, pH 4.5) containing Cu^{2+} (2 mM) and Ca^{2+} (5 mM), with their absorbance adjusted to the range of 0.9-1.0. The solutions were stored at + 4°C in the dark. The decolorization reaction was carried out using ~ 45 mg of the beads in freshly prepared dye solution (1 mL), in the dark, at room temperature, without agitation. All reactions were performed in triplicate. The decolorization process was monitored for 24 h from the addition of the dye solution. Aliquots were taken during the 24-hour period (every two hours for 12 h and one final aliquot after 24 h), and their absorbance was measured using an Elisa Microplate Reader at 620 nm. As a control, the absorbance of the dye solution prepared without the addition of the beads was also measured and the obtained values were subtracted from the values obtained using the beads with immobilized enzyme. After measuring the

initial absorbance (A initial) and final absorbance (A final), the percentage decolorization was calculated using the following formula:

Relative decolorization (%) = ((A initial-A final) / (A initial)) × 100%

The decolorization efficiency was expressed as residual decolorization, calculated relative to the decolorization degree of alginate with a lower degree of modification (2.5%) that was not photopolymerized, after 24 h, for each color.

Results and discussion

Yeast surface display of laccase

The gene for laccase from *Streptomyces cyaneus* CECT 3335 was successfully cloned into the pCTCON2 vector, and this construct was used for the successful transformation of competent *Saccharomyces cerevisiae* EBY100 cells. Individual colonies of the transformed yeast cells were utilized for the expression of laccase on the cell surface as a chimeric protein with the Aga2 protein. Induction of expression was performed in the presence of galactose, with an optimal expression time of 16 h, during which the highest level of expression and the greatest laccase activity using ABTS as a substrate were measured (Popović et al. 2021). Cu^{2+} ions are necessary for enzyme activation (Arias et al. 2003), as copper is located in the active site of laccase (Hakulinen & Rouvinen 2015) so they were added during each assay. To verify the success of laccase expression, the parallel transformation of yeast cells with the empty pCTCON2 vector was performed, and the efficiency of expression was examined under the same conditions using the same assay. The yeast cells transformed with the empty pCTCON2 vector did not exhibit any enzymatic activity. The advantage of laccase immobilized on yeast cell surface compared to the free enzyme lies in its reusability since it retains 88% of its activity after 6 cycles of dye removal, probably due to the increased stability caused by limiting conformational changes, especially at higher temperatures (Bertrand et al. 2016, Wu et al. 2020).

To increase the activity of laccase successfully expressed on the yeast cell surface, chemical lysis of the cells was performed using an organic solvent. The optimal conditions for cell lysis leading to the highest enzymatic activity were previously determined and involved a 24 h treatment with a 3% toluene solution in water at room temperature (Popović et al. 2021). This procedure resulted in the disruption of the cell wall, releasing the intracellular content and obtaining cell walls with attached laccase on the surface, whose activity was measured using ABTS as a substrate. After lysing, the specific activity of cell wall laccase increased significantly, from 0.035 ± 0.006 IU/g to 3.2 ± 0.2 IU/g (91 times).

Synthesis and spectral characterization of tyramine-alginate

The first step in alginate modification is periodate oxidation, with different degrees of oxidation (2.5, 5, 10, and 15 mol%) depending on the final concentration of metaperiodate. The resulting aldehyde groups are then subjected to reductive amination in the presence of tyramine hydrochloride and sodium

cyanoborohydride, leading to the formation of secondary amines (Fig. 1). The introduction of a new tyramine group into the structure of alginate opens up the possibility for additional chemical transformations and cross-linking reactions. Also, the reductive amination reaction led to the introduction of new positively charged groups into the structure of the molecule, preserving the carboxyl groups and increasing the total number of charged groups, which led to an increase in the solubility of the modified alginate and reduced solution viscosity. Only alginates with a degree of modification of 2.5 and 5 mol% were used for further experiments, while alginates with a higher degree of modification were not utilized due to the insufficient mechanical stability of the tyramine-alginate beads. The success of alginate modification and the degree of modification were confirmed by UV-Vis, FTIR, and 1H NMR spectroscopic methods. The UV-Vis spectrum was recorded in the wavelength range of 200 to 350 nm, and the difference in absorption between native and modified alginate was observed at around 280 nm. At this wavelength, the modified alginate showed an increased absorption peak, attributed to the introduction of the tyramine moiety into the structure, which has its absorption maximum at 280 nm, unlike native alginate which does not have an absorption maximum at this wavelength. Additionally, an increase in the intensity of the absorption peak was observed with a higher degree of modification, indicating the incorporation of more tyramine units into the structure, as mentioned in our previous work (Prodanovic et al. 2015).

Chemical modification was confirmed by spectral characterization in our previous research. The FT-IR spectra of tyramine-alginate showed the presence of aromatic rings, indicated by the peak at 1520 cm-1 corresponding to the C-C (in-ring) stretching vibration. This peak was observed only in the spectrum of modified alginate. The recorded 1H NMR spectra also confirmed the success of the modification, as evidenced by the presence of peaks corresponding to three aromatic hydrogen atoms at 6.7 ppm, which originate from the tyramine structure. These peaks were observed in the spectrum of tyramine-alginate, but not in the spectrum of native alginate (Prodanovic et al. 2015).

Immobilization of cell walls

The cell wall laccase was first immobilized within tyramine-alginate beads using a classical crosslinking with Ca^{2+} ions. The immobilization mixture, consisting of modified alginate and cell wall laccases, was added dropwise to a $CaCl_2$ solution while stirring, resulting in the instantaneous formation of mechanically stable spherical alginate beads. In our previous study, cell walls were immobilized within alginate-dopamine beads and the maximum specific enzymatic activity was achieved when a mixture containing 5 mol% dopamine-alginate and 150 mg/ml of the cell walls was dropped into a 2% (w/v) $CaCl_2$ solution (Popović et al. 2021). In this study, the optimum concentration of cell walls was 200 mg/mL, due to the different physicochemical characteristics of the hydrogels formed by alginate-dopamine and tyramine-alginate. As described in previous studies, the substitution of phenyl side groups with catechol groups leads to a remarkable enhancement of the adhesion properties. The adhesion strength of alginate-dopamine hydrogels is approximately ten times higher than that of tyramine-alginate hydrogels with an equal degree of substitution of 10% (Hou et al. 2015). The encapsulation of enzymes

in tyramine-alginate and alginate-dopamine macro-beads has not yet been directly compared. However, one can speculate that the encapsulation efficiency may be lower in tyramine-alginate due to the differences in the chemical structure of the hydrogels formed and the variations in the immobilization conditions. Based on its structure with more hydroxyl groups, alginate-dopamine has the potential to create more crosslinks and form more densely cross-linked hydrogels, thereby preventing potential enzyme leakage. This was confirmed by the fact that for the production of mechanically stable spherical beads from tyramine-alginate with 2.5 mol% substitution, a 1.8 times higher polymer concentration was required compared to native alginate. On the other hand, to produce beads using tyramine-alginate with 5 mol% substitution, the required concentration of tyramine-alginate was 2.1 times higher than that of the native polymer. However, there was no difference in the required concentration of alginate-dopamine and native alginate (Popović et al. 2021). Despite the increase in the concentration of immobilized cell walls with surface-displayed laccase in tyramine-alginate from 150 to 200 mg/mL, the specific laccase activity in alginate-dopamine was approximately two times higher (Popović et al. 2021) than in tyramine-alginate. This implies that there is enzyme leakage, necessitating additional crosslinking of the tyramine-alginate hydrogel to prevent it.

Photopolymerization of biocatalysts with visible light

Alginate hydrogels crosslinked by $CaCl_2$ often exhibit non-uniform and heterogeneous structures, resulting in relatively poor mechanical properties. This is attributed to the high mobility of Ca^{2+} ions in water, which can quickly form alginate hydrogel with a short gelation time. As a result, the ionic crosslinking occurs rapidly at the outer polymer region, and slowly progresses to the interior due to additional diffusional resistance of the gel layer formed at the surface (Kim et al. 2020). To prevent enzyme leakage and improve enzyme activity and stability, it was necessary to further crosslink tyramine-alginate gel and enhance additionally its mechanical properties. While conventional UV crosslinking is commonly employed in bioprinting natural hydrogels, there has been a growing demand for visible light-induced photocrosslinking, because previous studies have shown that UV radiation can cause protein and DNA damage causing decrease in protein activity, chromosomal instability in cells, and lead to apoptosis and cell death (Parsons &Goss 1978). In contrast, the visible light system demonstrated significantly higher cell viability (~ 90%), even at high light intensities of 50 and 100 mW/cm2. This highlights the potential of the visible light system as a milder method for enzyme and cell immobilization that can also be used for the biofabrication of living-cell-laden constructs (Lim et al. 2016). Visible light (green LED light, 550 nm) and a riboflavin photoinitiator were used to create a hydrogel by tyramine self-crosslinking. By absorbing light energy in the UV or visible range, riboflavin molecule is excited to a short-lived singlet state (1 RF, lifetime of 10 − 8 s), followed by a highly reactive and long-lived triplet state (3 RF*, lifetime of 10^{-2} s), which can react with substrates (Type I) or oxygen molecular species (Type II) and generate reactive oxygen species (ROS). The formed ROS induce the crosslinking of tyramine-alginate by forming a covalent bond between the phenolic groups of tyramine (Hong et al. 2019). The proposed mechanism of tyramine dimerization involves the formation of phenolic radicals, where more stable ring-residing phenoxy radicals dimerize to form the C-C bonded dimer, and a ring-residing radical

dimerizes with an oxygen-residing radical to form the less common C-O dimer (Hong et al. 2019, Hou et al. 2015, Nezhad-Mokhtari et al. 2019) (Fig. 2).

The gel mechanical properties were tuned by varying riboflavin concentration, incubation time in riboflavin solution, and visible-light exposure time. The beads were incubated in 0.005% and 0.01% (w/v) riboflavin solutions in sodium phosphate buffer (0.1M, pH = 6) for 15 minutes with stirring. At lower riboflavin concentrations and shorter incubation times, no photocross-linking occurred, while higher concentrations were not used to avoid initiator aggregation (Kim et al. 2020) and because of the generation of more harmful reaction products such as superoxide radicals ($O^{2\cdot}$) (Lim et al. 2016). It is expected that a higher concentration of the initiator will result in a greater number of radicals generated for the photopolymerization reaction. Additionally, when incubating alginate with different percentages of tyramine units, a higher concentration of riboflavin (0.01%) is expected to lead to increased efficiency of photopolymerization, resulting in enhanced activity of immobilized cell walls with laccase. Based on the obtained results (Fig. 3), it can be concluded that in the case of photopolymerization of 2.5 mol% alginate tyramine, the highest activity of immobilized cell walls with laccase, or the highest degree of crosslinking, was achieved by incubating the beads in a 0.005% riboflavin solution. However, for 5 mol% tyramine-alginate, the highest degree of crosslinking was obtained by incubating the beads in a 0.01% photoinitiator solution. In conclusion, the degree of alginate modification, more specifically the percentage of tyramine units in the modified alginate, determines the optimal riboflavin concentration for maximum crosslinking. The required polymerization time, or exposure time of the hydrogel to visible light, is dictated by the mechanical stability of the tyramine-alginate beads formed. The exposure time of 10 and 15 min did not result in additional crosslinking, while prolonged photopolymerization for more than 30 min caused the beads to swell with a significant increase in mass and volume, adversely affecting their mechanical properties and leading to cracking and fracturing of the beads.

Characterization of dual (ionically and photochemically with visible light) crosslinked tyramine-alginate beads

The photopolymerization of tyramine-alginate hydrogel was confirmed by FTIR spectroscopy. Analysis of the FTIR spectrum of the photopolymerized tyramine-alginate, based on the peaks at 1293 and 1213 cm^{-1} corresponding to the C-O-C asymmetric vibration in aryl ethers, provides confirmation of the proposed mechanism of photopolymerization by dimerization of tyramine through the formation of aryloxy radicals (Fig. 4). On the other hand, these two peaks were not observed in the non-photopolymerized beads. The peak shift from 1428 cm^{-1} in the non-photopolymerized hydrogel to 1412 cm^{-1} in the photopolymerized hydrogel can be attributed to extended conjugation, specifically the delocalization of π-electrons over both tyramine rings. This provides further evidence of the formation of a C-C bond and the coupling of the tyramine rings.

The effect of temperature on the enzymatic activity of immobilized cell walls with surface-displayed laccase

The temperature stability of free laccase cell walls and laccase cell walls immobilized in 2.5 and 5 mol% tyramine-alginate beads were determined by incubating the beads at the temperatures of 25, 30, 60, 65, and 80 ℃ for 1 h. Additionally, the effect of photopolymerization on the temperature stability of these beads was investigated under the same conditions. Enzyme activity was measured using ABTS as the substrate, as previously explained. As a control, immobilized cell walls of empty pCTCON2 were used, which did not show any activity. Free cell walls with surface displayed laccase showed the highest activity at 25 ℃. With an increase in temperature of just 5 ℃, they lost 43% of their activity. On the other hand, immobilized cell walls with surface displayed laccase not only exhibited better temperature stability, but also showed an increase in enzyme activity with temperature. The highest enzyme activity of immobilized cell walls was observed at 60 ℃, with a 109% increase in activity compared to 25 ℃. At 80 ℃, the immobilized cell walls retained 69% of their activity, while the free cell walls with surface-displayed laccase retained only 5% of their initial activity at 65 ℃. (Fig. 5.).

The enhanced stability of the immobilized laccase is attributed to the conformational flexibility of the molecules upon immobilization. Several other studies have reported high thermal stabilities of immobilized laccase at temperatures above 50°C (Hong et al. 2019, Nezhad-Mokhtari et al. 2019). In one study, the immobilized laccase retained 91% of its activity at 55 ℃ (Wang et al. 2010), but to the best of our knowledge, no study with immobilized laccase reported an increase in enzyme activity with increasing temperature. Increasing the temperature can lead to the rapid formation of enzyme-substrate complexes since the higher thermal energy of molecules results in increased mobility of both the enzyme and substrate molecules and, consequently, an increase in enzyme activity. Additionally, temperature can induce conformational changes in the enzyme, opening or stabilizing the active site, which allows better substrate accessibility. This can explain the observed increase in enzyme activity in the case of immobilized laccase cell walls. The enzyme activity of immobilized cell wall laccase in photopolymerized tyramine-alginate (2.5 mol% and 5 mol%) was significantly higher than the enzyme activity in non-photopolymerized hydrogel at all temperatures after 1 h of incubation, due to the additional crosslinking of the hydrogel. (Fig. 6).

The highest enzyme activity was observed at 60 ℃, with a 134% increase in activity for the 2.5 mol% tyramine-alginate photopolymerized beads, and a 130% increase in activity for the 5 mol% tyramine-alginate photopolymerized beads compared to the non-photopolymerized ones. As the immobilized enzyme exhibits the highest activity at 60 ℃, this incubation temperature was used to compare the enzymatic activity of immobilized laccase in alginate beads, tyramine-alginate beads with different degrees of alginate modification and the same beads photopolymerized under optimal conditions for each modified polymer (Fig. 7).

The enzyme immobilized in alginate beads exhibited the lowest activity, while the laccase immobilized in tyramine-alginate (5 mol%) beads showed a 161% increase in enzymatic activity compared to the laccase immobilized in tyramine-alginate (2.5 mol%) beads. The laccase immobilized in photopolymerized tyramine-alginate (5 mol%) beads exhibited a 104% increase in residual enzymatic activity compared to the laccase immobilized in photopolymerized tyramine-alginate (2.5 mol%) beads. Therefore, as the

degree of alginate modification with tyramine increases, a higher crosslinking density can be achieved by additional photochemical cross-linking. This results in greater thermal stability of the immobilized laccase, as demonstrated by the higher residual enzymatic activity. The enzymatic activity of the immobilized laccase in photopolymerized tyramine-alginate (5 mol%) beads is 2.46 times higher than the activity of the same immobilized laccase in alginate beads, at 60 ℃. The laccase immobilized in the photopolymerized hydrogel, after incubation at 60 ℃ for 6 h, retains 100% of its initial enzyme activity, which is a significant result compared to a previous study where laccase immobilized in magnetic mesoporous silica nanoparticles retained only 52% of its activity after incubation for 4 h at the same temperature (Wang et al. 2010).

The effect of pH on the enzymatic activity of immobilized cell wall laccase

The enzyme stability of cell wall laccase immobilized in different alginate hydrogels was determined by incubation in sodium-acetate buffer (0.1 M, pH 4.5) (Bagewadi et al. 2017, Popović et al. 2021, Wang et al. 2021) for 24 and 72 h at room temperature. The immobilized cell wall laccases in photopolymerized tyramine-alginate hydrogels exhibited higher stability compared to those immobilized in non-photopolymerized hydrogels. Figure 8 shows that after 72 h, the enzyme immobilized in photopolymerized hydrogels retained 100% of its activity, while the enzyme immobilized in 2.5 mol% tyramine-alginate retained 77% of its initial activity, and the enzyme immobilized in 5 mol% tyramine-alginate retained 82% of its initial activity.

After 21 days, the laccase immobilized in 5 mol% tyramine-alginate photopolymerized hydrogel retained 53% of its initial enzyme activity, while the same laccase immobilized in alginate hydrogel retained only 19% of its activity. Differences in the stability of laccase immobilized in hydrogels with different degrees of crosslinking are a result of variations in enzyme adsorption, dissociation, conformational changes, and its microenvironment. The preservation of laccase activity can be attributed to the dense hydrophobic network of dual ionic- and photo-crosslinked alginate, which reduces the detrimental effects of high temperature on the activity of immobilized enzymes (Wang et al. 2021).

Decolorization of synthetic dyes

The potential of immobilized cell wall laccase for the removal of synthetic dyes was investigated using photo-crosslinked and non-photo-crosslinked tyramine-alginate beads. Selected dyes from different groups were tested, including Remazol Brilliant Blue, Evans Blue, Amido Black 10B, Methylene Blue, and Guinea Green. The beads were incubated in the dye solutions for 24 h, and aliquots were taken every two hours to measure the absorbance and calculate the relative decolorization. The ability of control beads (beads with cell walls without laccase, containing empty pCTCON2 vector) to decolorize the dyes was also monitored to assess any dye adsorption onto the beads themselves. However, the control beads did not show any dye decolorization capability. Changes in the absorbance of dye solutions without biocatalysts were also measured under the same conditions. It was observed that only the Amido Black

10B dye degraded over 24 h, which was taken into account when calculating the relative decolorization by the biocatalysts Different hypothetical mechanisms of enzymatic dye Degradation were considered depending on the structure and the influence of electron-donating substituents, which promote successful degradation, as well as electron-withdrawing substituents, which can lead to reduced efficiency of decolorization through resonance destabilization (Legerska et al. 2016). The decolorization of all tested dyes was more efficient with photopolymerized biocatalysts as a result of additional polymer crosslinking and preservation of laccase activity (Fig. 9).

Compared to the previous study where no change in methyl green color was observed over 48 h in the presence of the photopolymerized biocatalyst, the relative decolorization of this dye is now 18.7% over 24 h (Fig. 9). The efficiency remained low due to the presence of two chloride ions per molecule, which are believed to participate in stabilizing the dye and reducing its susceptibility to degradation (Chmelová & Ondrejovič 2015). Additionally, the basic structure of methyl green is triphenylmethane (TPM), and it has been previously established that TPM-based dyes exhibit higher resistance to enzymatic degradation because laccases can oxidize the methyl carbon attached to TPM dye structure, giving stable products that are affected by p-substituted phenyl (Forootanfar et al. 2012). The same issue applies to Guinea Green, which also belongs to the class of TPM dyes. However, the efficiency of decolorization of Guinea Green (36.5% for 2.5 mol% Alg-Tyr and 65.4% for 5 mol% Alg-Tyr) using photopolymerized biocatalysts is higher than that of methyl green due to the presence of multiple electron-donating groups. The decolorization efficiency towards methylene blue is even higher because it belongs to the phenothiazine group of dyes with one chloride ion per molecule, but it is still lower compared to azo dyes and Remazol Brilliant Blue. The results presented in Fig. 9 shows that the highest degree of decolorization over 24 h was achieved for Evans Blue (75% for 2.5 mol% Alg-Tyr and 77.4% for 5 mol% Alg-Tyr) and Remazol Brilliant Blue (73.2% for 5 mol% Alg-Tyr) using photopolymerized biocatalysts. The mechanism of decolorization for azo dyes, such as Evans Blue and Amido Black, is similar. However, the less efficient decolorization of Amido Black (70% for 5 mol% Alg-Tyr photopolymerized) is due to the resonance effect of the $-NO_2$ group, particularly in the para position, and the presence of $-SO_3^{2-}$ in the ortho position. In our previous study, the maximum relative decolorization of these dyes (Evans Blue and Amido Black 10B) using non-photopolymerized dopamine-alginate biocatalysts was 60% (Pawar &Edgar 2012). Generally, anthraquinone dyes like Remazol Brilliant Blue are suitable substrates for laccase (Legerska et al. 2016). In the previous study, the decolorization efficiency of these dyes using immobilized laccase from M. thermophila was 60%, but only in the presence of a redox mediator (Daâssi et al. 2013). In our previous research, the decolorization efficiency of these dyes using immobilized laccase in dopamine-alginate beads without a redox mediator was 61% (Pawar &Edgar 2012).

Conclusions

Streptomyces cyaneus lacasse heterologously expressed within *S. cerevisiae* cell walls was immobilized within tyramine-modified alginate beads by dual crosslinking using Ca^{2+} ions and visible light photopolymerization. The higher crosslinking density of tyramine-alginate visible light photopolymerized

hydrogels led to a more compact hydrogel network structure with higher mechanical strength and smaller pore size compared to non-photopolymerized beads, yielding increased enzymatic activity, decreased enzyme leakage, and therefore more effective decolorization. Furthermore, cross-linking of the tyramine-alginate hydrogel by milder methods, such as visible light photopolymerization, not only better preserves enzymatic activity during immobilization but could also be very useful for keeping the viability of cells during 3D bioprinting in tissue engineering and other similar applications.

Statements and Declarations

Ethical approval Not applicable.

Consent to participate Not applicable.

Consent to publish Not applicable.

Author Contribution Conceptualization, R.P. and G.V.; methodology, D.J., A.S., and O.P..; validation, O.P., N.P.K, and D.J.; formal analysis, D.J. and N.P.K.; investigation, D.J., A.S. and M.C.P.; resources, R.P.; writing—original draft preparation, D.J.; writing—review and editing, R.P and G.V..; visualization, D.J.; supervision, R.P.; funding acquisition, R.P. All authors have read and agreed to the published version of the manuscript."

Funding This research was funded by the Ministry of Science, Technological Development and Innovation of the Republic of Serbia Grant No. 451-03-47/2023-01/200168 (University of Bel-grade-Faculty of Chemistry), Grant no. 451-03-47/2023-14/200288 (Innovative Centre of the Faculty of Chemistry) (RS-200288), Grant No. 451-03-47/2023-01/200053 (University of Belgrade-Institute for Multidisciplinary Research).

Competing interest The authors have no relevant financial or non-financial interests to disclose

Data availability All data underlying the results are available as part of the article and no additional source date are required.

References

1. Arias ME, Arenas M, Rodríguez J, Soliveri J, Ball Andrew S, Hernández M (2003) Kraft Pulp Biobleaching and Mediated Oxidation of a Nonphenolic Substrate by Laccase from *Streptomyces cyaneus* CECT 3335. Appl Environ Microbiol 69:1953–1958. https://doi.org/10.1128/AEM.69.4.1953-1958.2003
2. Bagewadi ZK, Mulla SI, Ninnekar HZ (2017) Purification and immobilization of laccase from Trichoderma harzianum strain HZN10 and its application in dye decolorization. J genetic Eng Biotechnol 15:139–150. https://doi.org/10.1016/j.jgeb.2017.01.007

3. Bertrand B, Trejo-Hernández MR, Morales-Guzmán D, Caspeta L, Suárez Rodríguez R, Martínez-Morales F (2016) Functional expression, production, and biochemical characterization of a laccase using yeast surface display technology. Fungal biology 120:1609–1622. https://doi.org/10.1016/j.funbio.2016.08.009
4. Bilal M, Adeel M, Rasheed T, Zhao Y, Iqbal HMN (2019) Emerging contaminants of high concern and their enzyme-assisted biodegradation – A review. Environ Int 124:336–353. https://doi.org/10.1016/j.envint.2019.01.011
5. Brown MA, De Vito SCJCries technology (1993) Predicting azo dye toxicity. 23:249–324. http://dx.doi.org/10.1080/10643389309388453
6. Bryant SJ, Nuttelman CR, Anseth KS (2000) Cytocompatibility of UV and visible light photoinitiating systems on cultured NIH/3T3 fibroblasts in vitro. J Biomater Sci Polym Ed 11:439–457. https://doi.org/10.1163/156856200743805
7. Chen M, Bolognesi G, Vladisavljević GT (2021) Crosslinking Strategies for the Microfluidic Production of Microgels. 26:3752. https://doi.org/10.3390/molecules26123752
8. Chiulan I, Heggset EB, Voicu ŞI, Chinga-Carrasco G (2021) Photopolymerization of Bio-Based Polymers in a Biomedical Engineering Perspective. Biomacromolecules 22:1795–1814. https://doi.org/10.1021/acs.biomac.0c01745
9. Chmelová D, Ondrejovič M (2015) Effect Of Metal Ions On Triphenylmethane Dye Decolorization By Laccase From Trametes Versicolor. Nova Biotechnol et Chim 14:191–200. https://doi.org/10.1515/nbec-2015-0026
10. Daâssi D, Mechichi T, Rodriguez-Couto S (2013) Decolorization of the metal textile dye Lanaset Grey G by immobilized white-rot fungi. J Environ Manage 129C:324–332. https://doi.org/10.1016/j.jenvman.2013.07.026
11. Daâssi D, Rodríguez-Couto S, Nasri M, Mechichi T (2014) Biodegradation of textile dyes by immobilized laccase from Coriolopsis gallica into Ca-alginate beads. Int Biodeterior Biodegrad 90:71–78. https://doi.org/10.1016/j.ibiod.2014.02.006
12. Dahle J, Kvam E, Stokke T (2005) Bystander effects in UV-induced genomic instability: antioxidants inhibit delayed mutagenesis induced by ultraviolet A and B radiation. J Carcinog 4:11. https://doi.org/10.1186/1477-3163-4-11
13. Donnelly PE, Chen T, Finch A, Brial C, Maher SA, Torzilli PA (2017) Photocrosslinked tyramine-substituted hyaluronate hydrogels with tunable mechanical properties improve immediate tissue-hydrogel interfacial strength in articular cartilage. J Biomater Sci Polym Ed 28:582–600. https://doi.org/10.1080/09205063.2017.1289035
14. Fernández-Fernández M, Sanromán M, Moldes D (2013) Recent developments and applications of immobilized laccase. Biotechnol Adv 31:1808–1825. https://doi.org/10.1016/j.biotechadv.2012.02.013
15. Forootanfar H, Moezzi A, Aghaie-Khozani M, Mahmoudjanlou Y, Ameri A, Niknejad F, Faramarzi MA (2012) Synthetic dye decolorization by three sources of fungal laccase. Iran J Environ health Sci Eng

9:27. https://doi.org/10.1186/1735-2746-9-27

16. Hakulinen N, Rouvinen J (2015) : Three-dimensional structures of laccases. Cellular and molecular life sciences: CMLS 72, 857 – 68. https://doi.org/10.1007/s00018-014-1827-5
17. Higham AK, Bonino CA, Raghavan SR, Khan SA (2014) Photo-activated ionic gelation of alginate hydrogel: real-time rheological monitoring of the two-step crosslinking mechanism. Soft Matter 10:4990–5002. https://doi.org/10.1039/C4SM00411F
18. Hoegger PJ, Kilaru S, James TY, Thacker JR, Kües U (2006) Phylogenetic comparison and classification of laccase and related multicopper oxidase protein sequences. FEBS J 273:2308–2326. https://doi.org/10.1111/j.1742-4658.2006.05247.x
19. Hong B, Park S, Park WH (2019) Effect of photoinitiator on chain degradation of hyaluronic acid. Biomaterials Res 23. https://doi.org/10.1186/s40824-019-0170-1
20. Hou J, Li C, Guan Y, Zhang Y, Zhu XX (2015) Enzymatically crosslinked alginate hydrogels with improved adhesion properties. Polym Chem 6:2204–2213. https://doi.org/10.1039/C4PY01757A
21. Hsueh C-C, Chen B-Y, Yen C-Y (2009) Understanding effects of chemical structure on azo dye decolorization characteristics by Aeromonas hydrophila. J Hazard Mater 167:995–1001. https://doi.org/10.1016/j.jhazmat.2009.01.077
22. Khan R, Bhawana P, Fulekar MH (2013) Microbial decolorization and degradation of synthetic dyes: a review. Reviews in Environmental Science and Bio/Technology 12:75–97. https://doi.org/10.1007/s11157-012-9287-6
23. Kim E, Kim MH, Song JH, Kang C, Park WH (2020) Dual crosslinked alginate hydrogels by riboflavin as photoinitiator. Int J Biol Macromol 154:989–998. https://doi.org/10.1016/j.ijbiomac.2020.03.134
24. Kim S-h, Chu C-C (2009) Visible light induced dextran-methacrylate hydrogel formation using (–)-riboflavin vitamin B2 as a photoinitiator and L-arginine as a co-initiator. Fibers Polym 10:14–20. https://doi.org/10.1007/s12221-009-0014-z
25. Kong X, Mohanty SK, Stephens J, Heale JT, Gomez-Godinez V, Shi LZ, Kim JS, Yokomori K, Berns MW (2009) Comparative analysis of different laser systems to study cellular responses to DNA damage in mammalian cells. Nucleic Acids Res 37:e68. https://doi.org/10.1093/nar/gkp221
26. Lee KY, Mooney DJ (2001) Hydrogels for tissue engineering. Chem Rev 101:1869–1879. https://doi.org/10.1021/cr000108x
27. Lee KY, Mooney DJ (2012) Alginate: Properties and biomedical applications. Prog Polym Sci 37:106–126. https://doi.org/10.1016/j.progpolymsci.2011.06.003
28. Legerska B, Chmelová D, Ondrejovič M (2016) : Degradation of Synthetic Dyes by Laccases – A Mini-Review. Nova Biotechnologica et Chimica 15. https://doi.org/10.1515/nbec-2016-0010
29. Li K, Xu F, Eriksson KE (1999) Comparison of fungal laccases and redox mediators in oxidation of a nonphenolic lignin model compound. Appl Environ Microbiol 65:2654–2660. https://doi.org/10.1128/aem.65.6.2654-2660.1999

30. Lim KS, Schon BS, Mekhileri NV, Brown GCJ, Chia CM, Prabakar S, Hooper GJ, Woodfield TBF (2016) New Visible-Light Photoinitiating System for Improved Print Fidelity in Gelatin-Based Bioinks. ACS Biomater Sci Eng 2:1752–1762. https://doi.org/10.1021/acsbiomaterials.6b00149
31. Mate DM, Alcalde M (2017) Laccase: a multi-purpose biocatalyst at the forefront of biotechnology. Microb Biotechnol 10:1457–1467. https://doi.org/10.1111/1751-7915.12422
32. Mishbak HH, Cooper G, Bartolo PJ (2019) Development and characterization of a photocurable alginate bioink for three-dimensional bioprinting. Int J bioprinting 5:189. https://doi.org/10.18063/ijb.v5i2.189
33. Nezhad-Mokhtari P, Ghorbani M, Roshangar L, Soleimani Rad J (2019) Chemical gelling of hydrogels-based biological macromolecules for tissue engineering: Photo- and enzymatic-crosslinking methods. Int J Biol Macromol 139:760–772. https://doi.org/10.1016/j.ijbiomac.2019.08.047
34. Noshadi I, Hong S, Sullivan KE, Shirzaei Sani E, Portillo-Lara R, Tamayol A, Shin SR, Gao AE, Stoppel WL, Black Iii LD, Khademhosseini A, Annabi N (2017) In vitro and in vivo analysis of visible light crosslinkable gelatin methacryloyl (GelMA) hydrogels. Biomaterials Sci 5:2093–2105. https://doi.org/10.1039/C7BM00110J
35. Pawar SN, Edgar KJ (2012) Alginate derivatization: a review of chemistry, properties and applications. Biomaterials 33 3279 – 305. https://doi.org/10.1016/j.biomaterials.2012.01.007
36. Popli S, Patel UD (2015) Destruction of azo dyes by anaerobic–aerobic sequential biological treatment: a review. Int J Environ Sci Technol 12:405–420. https://doi.org/10.1007/s13762-014-0499-x
37. Popović N, Pržulj D, Mladenović M, Prodanović O, Ece S, Ilić Đurđić K, Ostafe R, Fischer R, Prodanović R (2021) Immobilization of yeast cell walls with surface displayed laccase from *Streptomyces cyaneus* within dopamine-alginate beads for dye decolorization. Int J Biol Macromol 181:1072–1080. https://doi.org/10.1016/j.ijbiomac.2021.04.115
38. Prodanovic O, Spasojevic D, Prokopijevic M, Radotic K, Markovic N, Blazic M, Prodanovic R (2015) Tyramine modified alginates via periodate oxidation for peroxidase induced hydrogel formation and immobilization. Reactive and Functional Polymers 93:77–83. https://doi.org/10.1016/j.reactfunctpolym.2015.06.004
39. Sakai S, Hashimoto I, Ogushi Y, Kawakami K (2007) Peroxidase-catalyzed cell encapsulation in subsieve-size capsules of alginate with phenol moieties in water-immiscible fluid dissolving H2O2. Biomacromolecules 8:2622–2626. https://doi.org/10.1021/bm070300
40. Shanmugam S, Basha C, Perumalsamy M, Prabhu H (2012) Electrochemical oxidation and aerobic biodegradation with isolated bacterial strains for dye wastewater: Combined and integrated approach. Electrochim Acta 77:171–178. https://doi.org/10.1016/j.electacta.2012.05.084
41. Shokri Z, Seidi F, Karami S, Li C, Saeb MR, Xiao H (2021) Laccase immobilization onto natural polysaccharides for biosensing and biodegradation. Carbohydr Polym 262:117963. https://doi.org/10.1016/j.carbpol.2021.117963

42. Stolz A (2001) Basic and applied aspects in the microbial degradation of azo dyes. Appl Microbiol Biotechnol 56:69–80. https://doi.org/10.1007/s002530100686
43. Strong J, Claus H (2011) Laccase: A Review of Its Past and Its Future in Bioremediation. Crit Reviews Environ Sci Technol - CRIT REV ENVIRON SCI TECHNOL 41:373–434. https://doi.org/10.1080/10643380902945706
44. Taheri-Kafrani A, Kharazmi S, Nasrollahzadeh M, Soozanipour A, Ejeian F, Etedali P, Mansouri-Tehrani HA, Razmjou A, Yek SM, Varma RS (2021) Recent developments in enzyme immobilization technology for high-throughput processing in food industries. Crit Rev Food Sci Nutr 61:3160–3196. https://doi.org/10.1080/10408398.2020.1793726
45. Uygun M, Asunción-Nadal Vdl, Evli S, Uygun DA, Jurado-Sánchez B, Escarpa A (2021) Dye removal by laccase-functionalized micromotors. Appl Mater Today 23:101045. https://doi.org/10.1016/j.apmt.2021.101045
46. Wang F, Guo C, Yang L, Liu C-Z (2010) Magnetic mesoporous silica nanoparticles: Fabrication and their laccase immobilization performance. Bioresour Technol 101:8931–8935. https://doi.org/10.1016/j.biortech.2010.06.115
47. Wang Z, Ren D, Jiang S, Yu H, Cheng Y, Zhang S, Zhang X, Chen W (2021) The study of laccase immobilization optimization and stability improvement on CTAB-KOH modified biochar. BMC Biotechnol 21:47. https://doi.org/10.1186/s12896-021-00709-3
48. Wu Y, Chen Y, Wei N (2020) Biocatalytic properties of cell surface display laccase for degradation of emerging contaminant acetaminophen in water reclamation. Biotechnol Bioeng 117:342–353. https://doi.org/10.1002/bit.27214
49. Zhou W, Zhang W, Cai Y (2021) Laccase immobilization for water purification: A comprehensive review. Chem Eng J 403:126272. https://doi.org/10.1016/j.cej.2020.126272

Figures

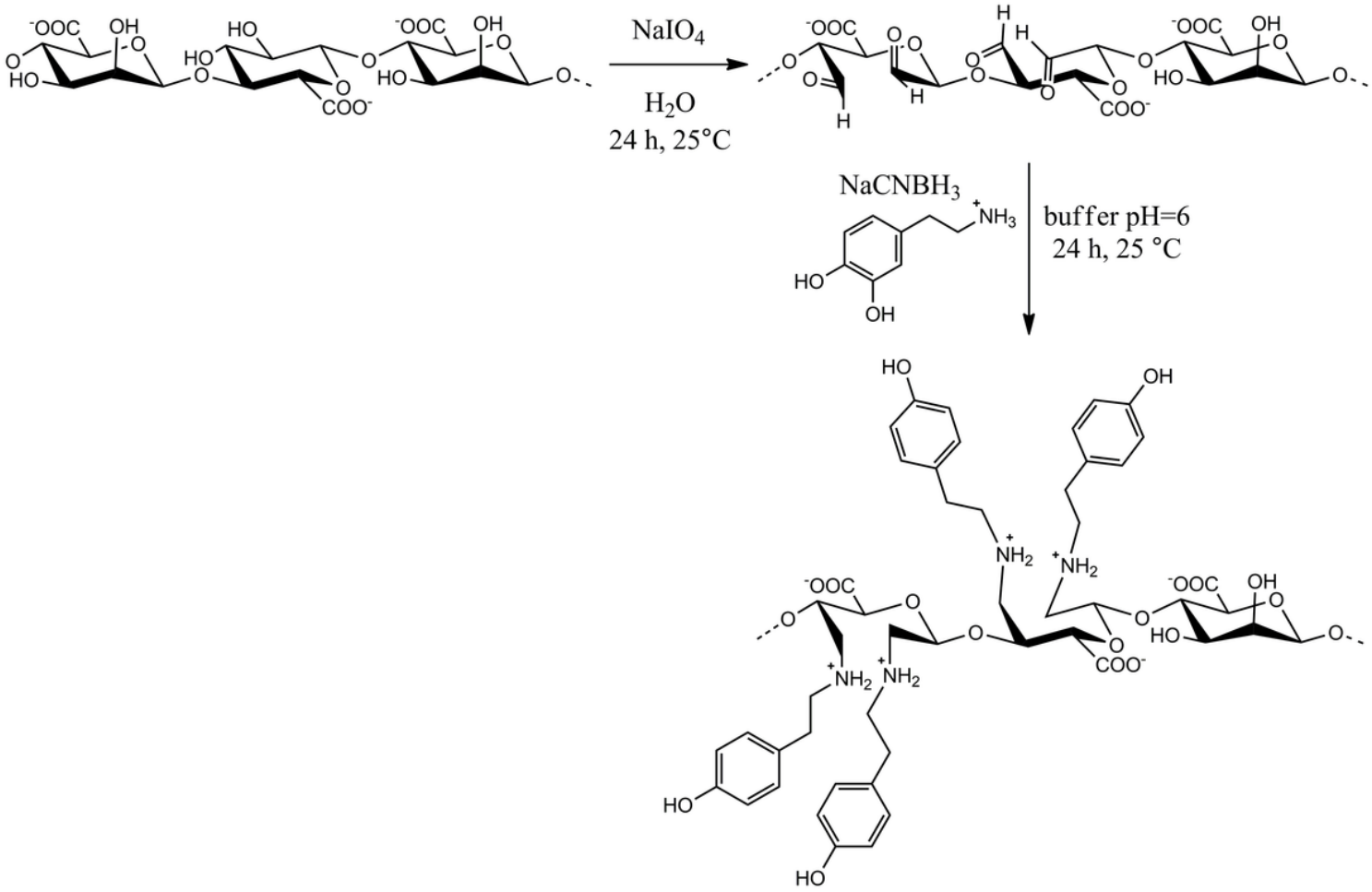

Figure 1

Synthesis of tyramine-alginate by periodate oxidation and reductive amination reactions

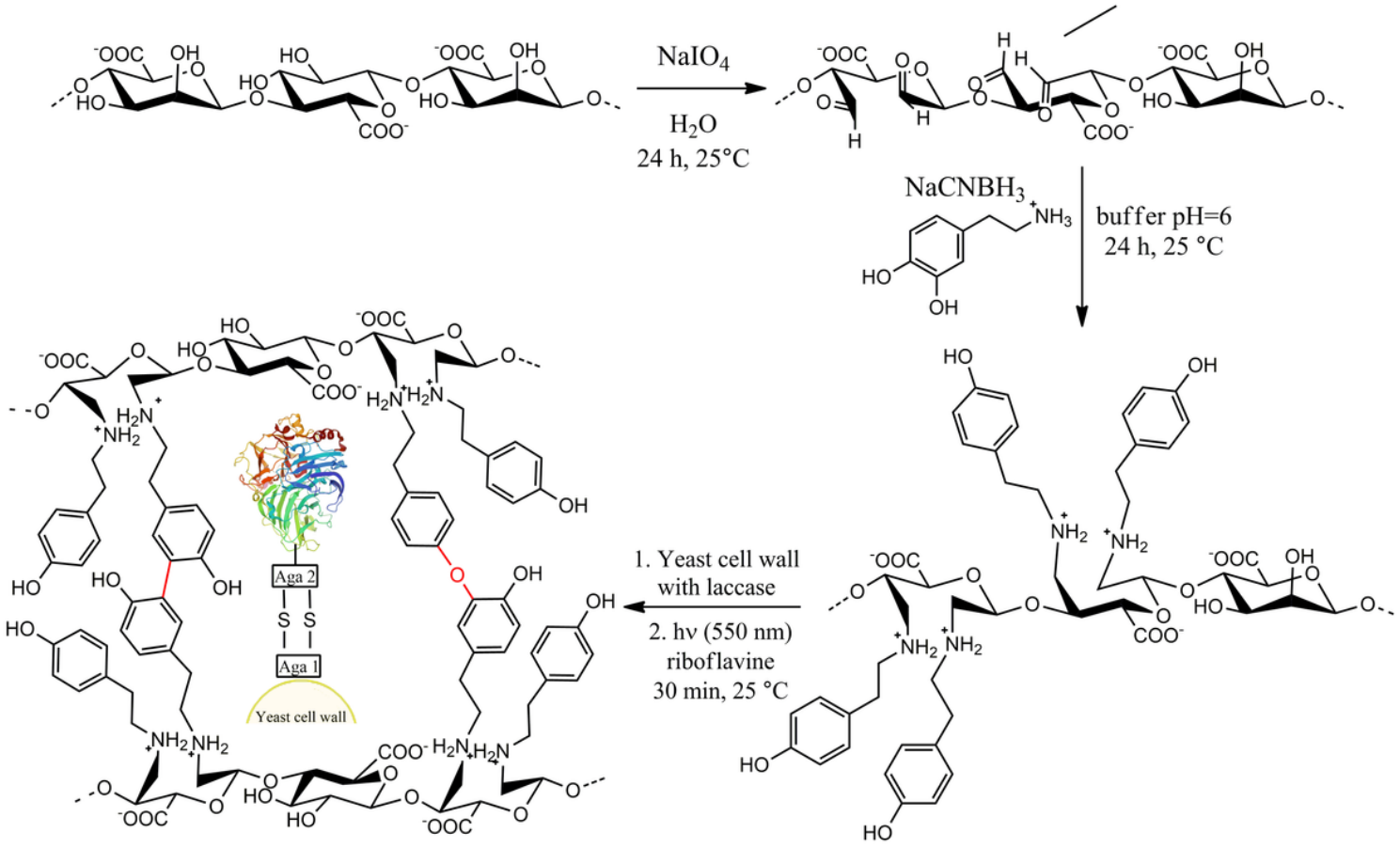

Figure 2

The proposed mechanism of photocrosslinking of tyramine-alginate in the presence of riboflavin as photoinitiator and the immobilization of cell walls with surface displayed laccase

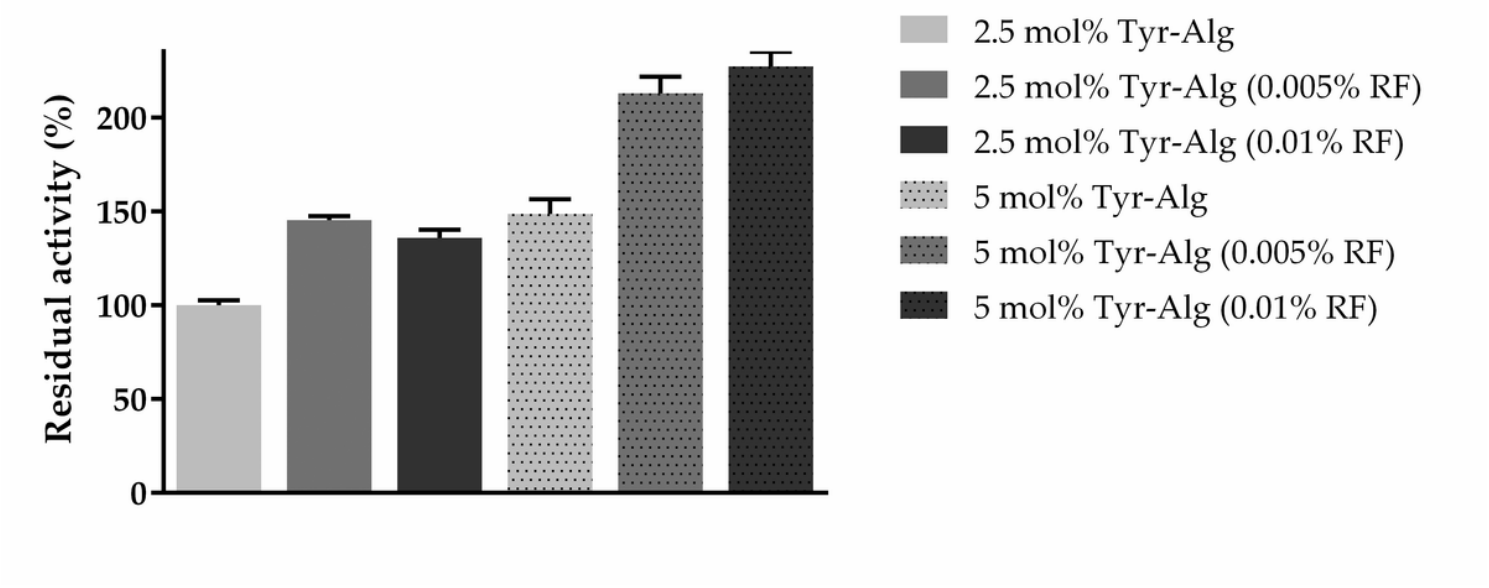

Figure 3

The residual activities of cell walls with surface displayed laccase immobilized in 2.5 mol% and 5 mol% tyramine-alginate, incubated in riboflavin (RF) solution of different concentrations

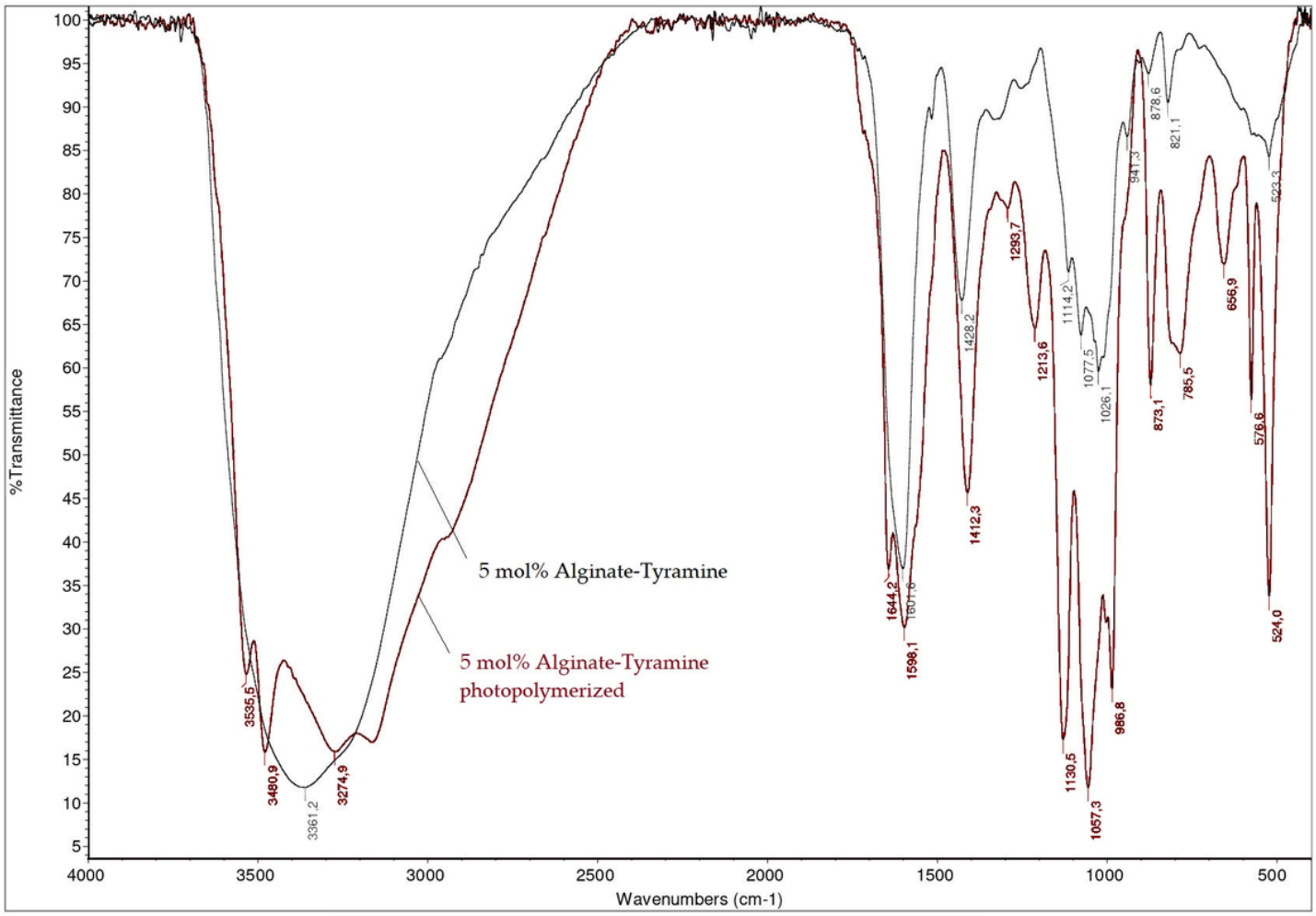

Figure 4

FTIR spectra of non-photopolymerized and photopolymerized tyramine-alginate. In both cases, the degree of polymer oxidation was 5 mol%

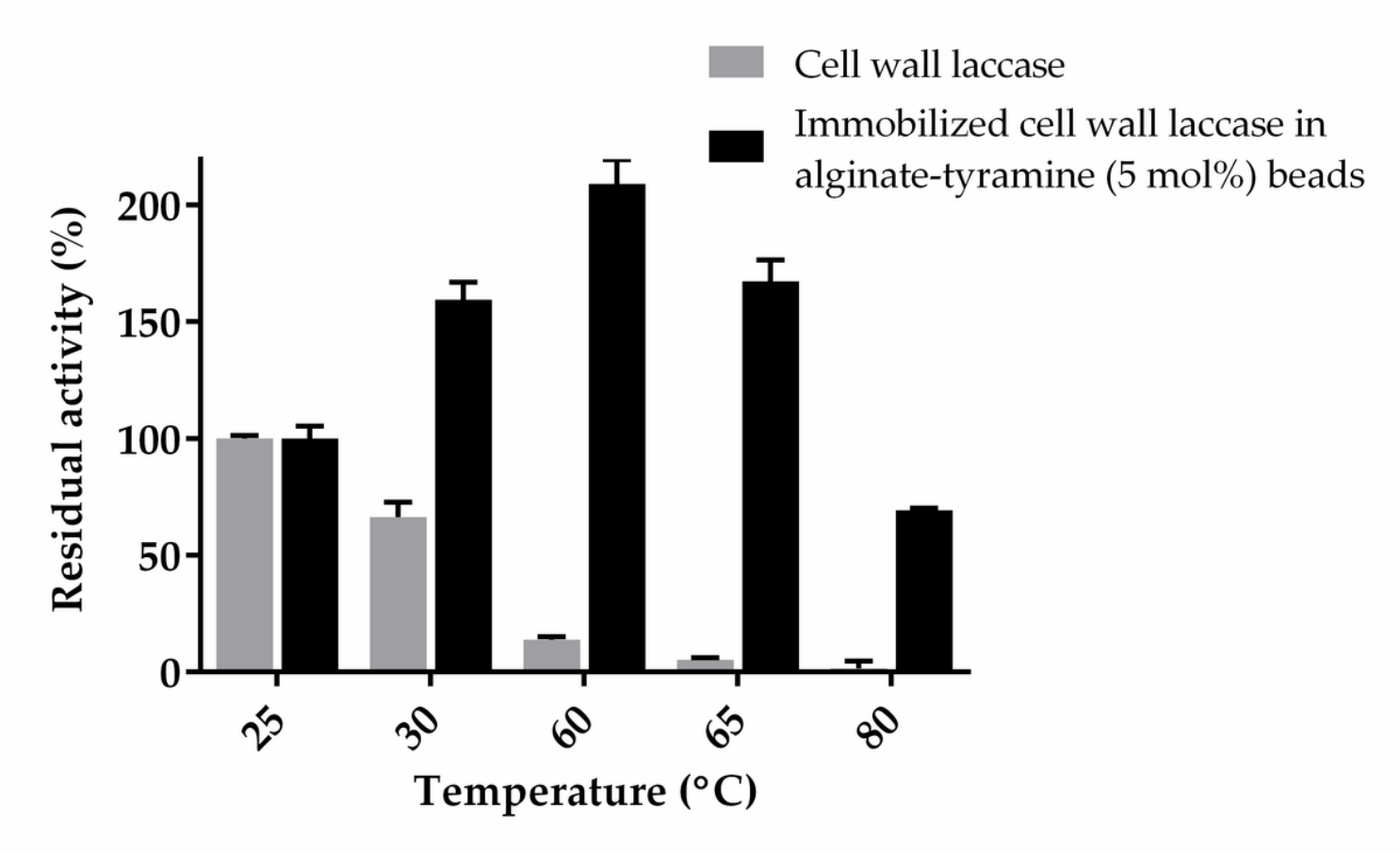

Figure 5

The temperature stability of free and immobilized laccase represented by the residual activity achieved after 1 hour of incubation at 25, 30, 60, 65, and 80 ^{o}C

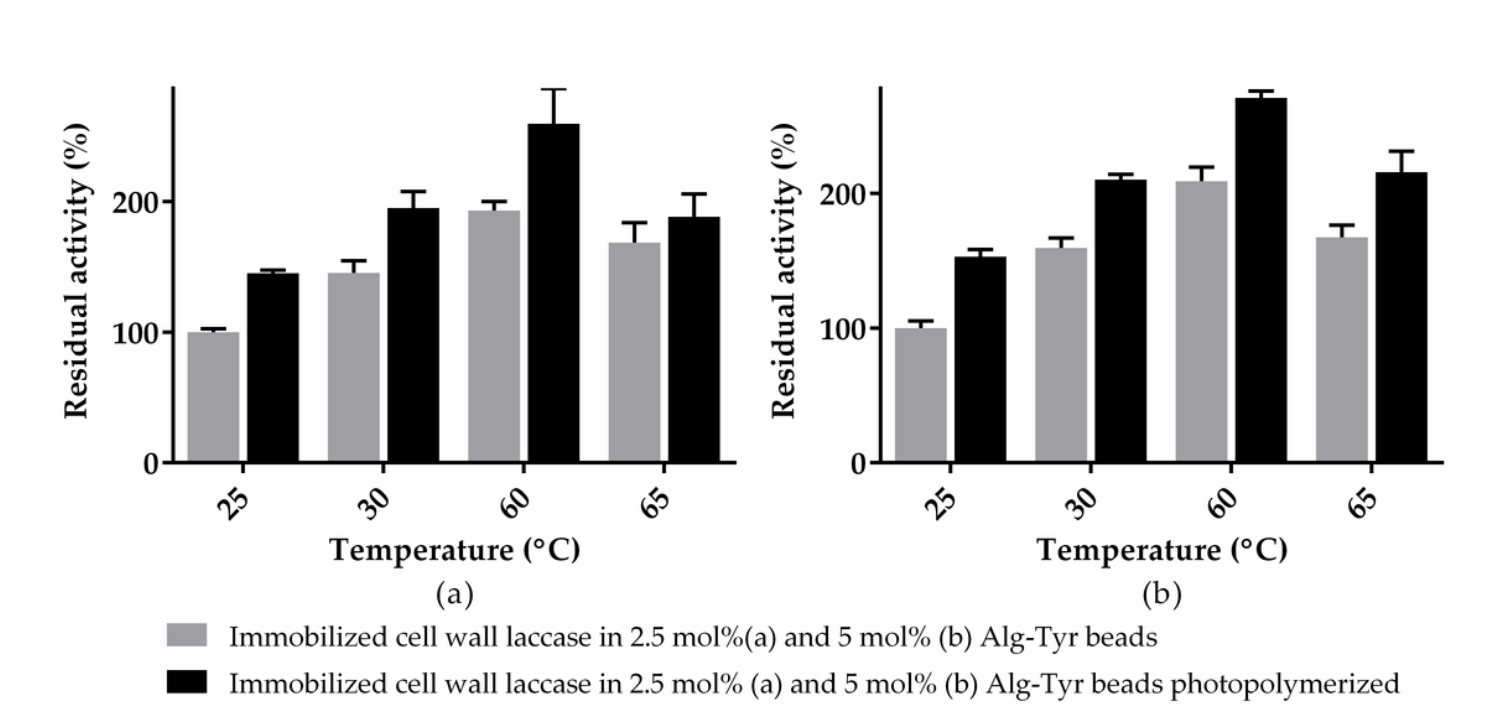

Figure 6

The temperature stability of immobilized laccase in non-photopolymerized and photo-polymerized tyramine-alginate beads represented by the residual activity after 1 h incubation at 25, 30, 60, and 65 °C

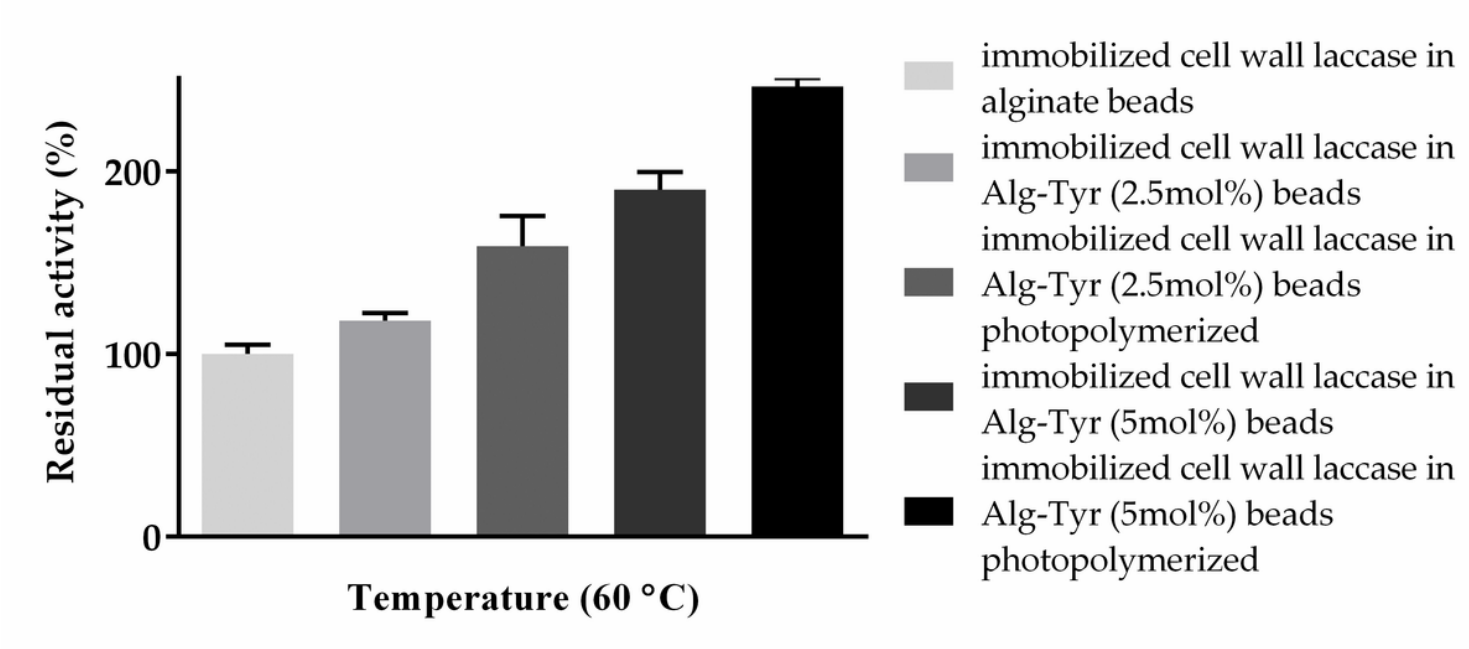

Figure 7

The temperature stability of immobilized laccase in alginate and tyramine-alginate beads (non-photopolymerized and photopolymerized) represented by the residual activity after 1 h of incubation at 60 °C

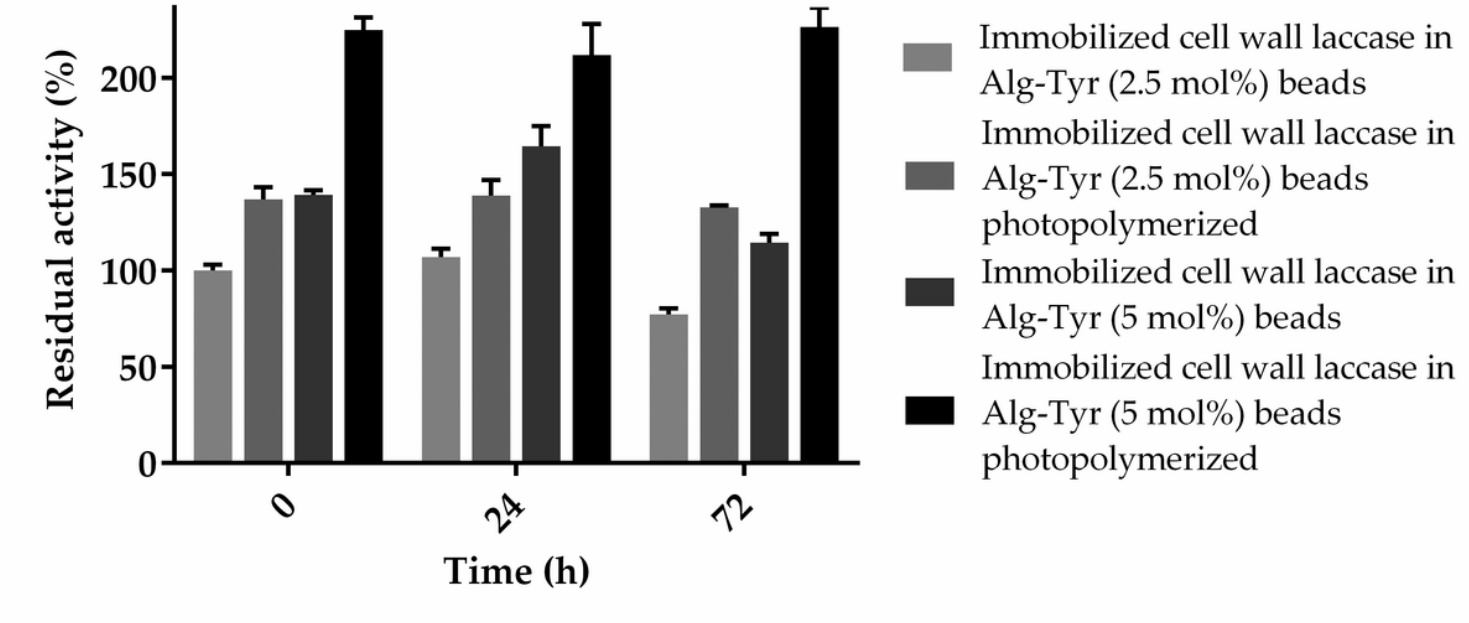

Figure 8

The pH stability of immobilized cell wall laccase in tyramine-alginate beads (photopolymerized and non-photopolymerized), after 24 and 72 h of incubation in optimal buffer

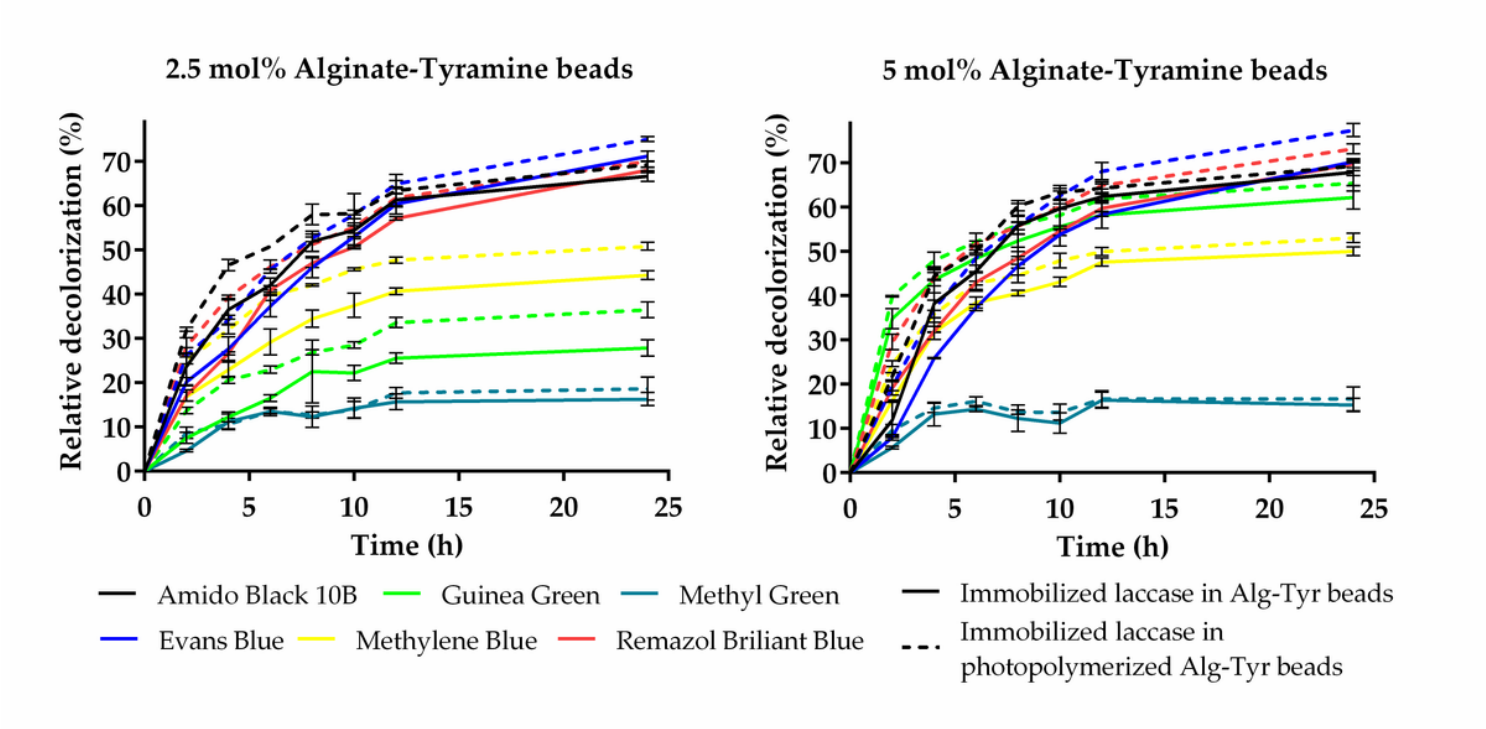

Figure 9

Time course of decolorization reaction (during 24 h) of several dyes: Evans Blue, Remazol Brilliant Blue, Amido Black 10B, Methylene Blue, Guinea Green